JOURNAL OF MATERIALS SCIENCE 28 (1993) 4391–4397

Mechanical characterization of fibres used for reinforcing metals and evaluation of seeded sol–gel derived alumina-fibre reinforced 1100 aluminium castings

C. M. LESCA,
Societa Italiana Resine, Montedison Via Bellini 35, Macherio, MI 20050, Italy

J. A. CORNIE
Department of Materials Science and Engineering, Massachusetts, Institute of Technology, Room 8-401, Cambridge, MA 02139, USA

J. B. FRILER, A. S. ARGON
Department of Mechanical Engineering, Massachusetts Institute of Technology, Room 1-306, Cambridge, MA 02139, USA

The properties of a newly developed seeded sol–gel-derived alumina fibre have been evaluated and compared with currently commercially available alumina and pitch-derived carbon fibres of similar modulus. These fibres were wrapped into preforms and pressure infiltration cast to form commercially-pure-aluminium (1100) matrix composites. The manufactured composites were then flexure and tensile tested to determine their axial and transverse properties. Calculations of the composite strength based upon the statistical theory of fracture were performed and are in good agreement with the experimental results.

1. Introduction

The attractive properties of fibrous metal matrix composites are derived directly from the properties of the reinforcement. For this reason, new reinforcements or production technologies that can increase the final mechanical properties of metal matrix composites are of great interest to the MIT Inorganic Composites Laboratory.

A new alumina fibre derived from a seeded sol–gel precursor has recently been made available by the 3M company and is in the process of being evaluated by the Inorganic Composites Laboratory at MIT. The fibre, with a diameter of about 10 μm, is polycrystalline with a grain size of the order of 40 nm [1]. Since this fibre has not been extensively evaluated outside the laboratories of the developer, the initial aim of our research has been the characterization of the variability of the strength and diameter of the fibre. The strength of the fibre was measured by single-filament tensile testing. In order to have results comparable with other fibres at more mature states of development, Weibull distributions of other commercially available fibres for the reinforcement of aluminium alloy matrices were obtained using the same testing techniques. Once the strength and strength distribution of the fibre lot provided by the manufacturer was evaluated, the next phase of the evaluation was the preparation of aluminium-matrix-composite specimens and the characterization of longitudinal and transverse tensile properties. Since only a limited amount of fibre was available, only a few specimens were prepared. The results discussed below should be considered as preliminary.

Two specimens containing 55% of the SSG (seeded sol–gel) alumina fibres were manufactured by pressure infiltration of commercial purity aluminium (1100) into a fibrous preform. Longitudinal tensile properties were determined by standard four-point bend tests. A second sample with the same volume fraction of Al_2O_3 fibres was evaluated by transverse tensile testing. Fracture surfaces were evaluated by scanning electron microscopy SEM and optical metallography.

2. Experimental techniques

2.1. Fibre testing

Single-filament tensile tests were performed by epoxy gluing a single fibre to a heavy-gauge paper card with a 2.54 cm cut-out window. Once the epoxy was cured, the fibre diameter was measured and the card was mounted in an Instron machine. The side frame of the cardboard window was cut and the fibre was loaded at a cross-head speed of 0.01 mm min^{-1}. The test machine was fitted with a 1 kg load cell.

Since the 3M seeded SSG fibre is a recent innovation and is in an early stage of development, it was

0022–2461

decided to co-evaluate more mature fibres as a comparison and to illuminate areas for further development by the manufacturer. The zirconia-stabilized alumina fibre PRD-166 manufactured by Du Pont and the pitch-base carbon fibre P-55 manufactured by AMOCO were selected. The PRD-166 fibre is larger in diameter (20 μm) than the SSG fibre, and is produced by a slurry-spinning technique. The grain size of the PRD-166 fibre is an order of magnitude larger than the SSG fibre, approximately 0.5 μm [2]. This, of course, results in a lower fibre strength. The P-55 fibres are about the same diameter as the SSG fibre and are produced by a similar technology, i.e. spinning from a pitch precursor.

Statistical scatter in strength values is observed for all materials and especially for ceramics and fibres. This variability can be evaluated by statistical description of the fibre strength. Experimental data can be described by a cumulative probability-distribution function denoted by $P(\sigma)$. The Weibull function used here can be written as [3]

$$P(\sigma) = 1 - \exp[-\Omega^*(\sigma - \sigma_u/\sigma_0)^m] \quad (1)$$

where σ_u is the lower limiting strength, σ_0 is a scale parameter, Ω is equal to the length of the fibre divided by the diameter and m is a parameter useful in describing the scatter of data which is usually called the Weibull modulus. σ_0 can also be considered to be the fundamental strength of the defect-free material. In Equation 1 the measurable quantities are the strength of a particular sample, σ, and $\Omega = 1/d$.

$P(\sigma)$ can be estimated from a large group of N samples, considering the n samples that have fractured at a stress of σ or less, using

$$\ln\{\ln[1/1 - P(\sigma)]\} = [\ln\Omega - m\ln\sigma_0] + m\ln\sigma \quad (2)$$

By a linear regression of the experimental data, it is possible to calculate the value of the Weibull modulus, m, and the parameter σ_0. The average strength, $\bar{\sigma}$, of a group of fibres is given by

$$\bar{\sigma} = \sigma_0\Omega^{-1/m}\Gamma[(m+1)/m] \quad (3)$$

where Γ is the tabulated gamma function; and the variance of σ, denoted by var(σ), which is equal to the square of the standard deviation S, is given by

$$\sigma^2 = \text{var}(\sigma) = \sigma_0^2\Omega^{-2/m}\{\Gamma[(m+2)/m] - \Gamma^2[(m+1)/m]\} \quad (4)$$

2.2. Infiltration casting of composite test specimens

Composite samples were obtained by pressure infiltration of molten metal into a SSG fibrous preform. The preforms used in this study were manufactured by filament winding and a cryopacking technique first developed by Dunand at MIT. This process is shown in Fig. 1. The aligned fibres on the wrapping mandrel were soaked with distilled water and frozen so that they could be cut, removed, and placed in the preforming mould. The dimensions of the mould were co-ordinated with the number of fibre wraps required to result in a 55 technique first developed by Dunand at MIT. This process is also shown in Fig. 1. The aligned fibres on the wrapping mandrel were soaked with distilled water and frozen so that they could be cut, removed, and placed in the preforming mould. The dimensions of the mould were co-ordinated with the number of fibre wraps required to result in 55 v/o volume fraction of reinforcement in the final preform. The fibres were resoaked with distilled water and refrozen to produce an ice-matrix composite which can be easily handled or stored prior to loading into the mould. The water is vaporized and removed by heating to the preheat temperature for at least 1 h at ~ 600 °C prior to infiltration.

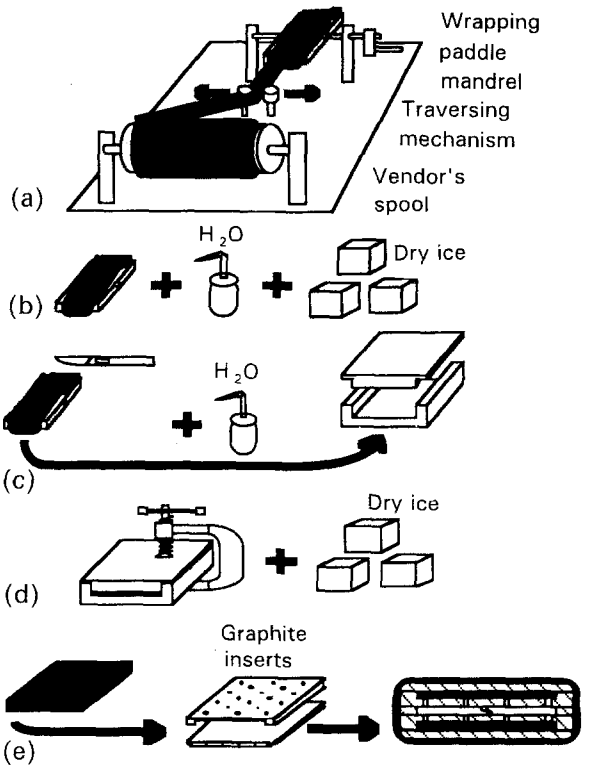

Figure 1 Preform fabrication and mould loading techniques. (a) The fibres are taken from the tow and wrapped onto the mandrel. (b) The wrapped mandrel is doused with water and frozen with dry ice. (c) The fibre preform is cut at the ends of the frozen wrapped madrel, inserted in the aluminium sizing-press, thawed, compressed to 55 v/o fraction; and (d) refrozen into a cryopacked preform. (e). Two cyropacked preforms are then loaded into the mould and weld sealed for preheating, outgassing and pressure infiltration.

During the metal-infiltration process, the mould loaded with the preform was placed at the bottom of a quartz tube closed at the end as shown in Fig. 2. The metal is placed at the top of the mould and is separated by a filter, a graphite spacer tube and a lower filter which provides thermal isolation between the melt and the preform. By using this technique, it was possible to independently control the melt and preform temperatures. This control is necessary for the production of high-quality castings, especially in systems where it is desirable to limit the fibre contact with the molten alloy due to chemical reactivity at the fibre–matrix interface. Processing temperatures were controlled and monitored by type-K thermocouples

located in protective wells in the melt, in the preform region and outside the mould vessel as shown in Fig. 2. The processing parameters used for the infiltration of the SSG fibrous preforms with 1100 aluminium are listed in Table I.

Two uniaxial $80 \times 5 \times 3$ mm specimens with a volume fraction of 0.55 were cast to near net shape for flexure testing. The two specimens were given a final surface machining to provide defect-free surfaces for testing.

2.3. Testing of composite specimens

2.3.1. Longitudinal strength

The axial tensile strength of the composite specimens was evaluated using a four-point bend fixture mounted on an Instron machine with a 1000 lb load-cell. The cross-head speed was 0.01 inch min^{-1}. All the tests were performed at room temperature. The test geometry and measured values are given in Table II.

2.3.2. Transverse strength

The transverse strength was tested in tension using the same Instron machine at room temperature and at a cross-head speed of 0.01 inch min^{-1}. The sample had a rectangular cross-section of 10×3 mm and a length of 90 mm.

3. Discussion of results

3.1. Fibre strength distribution

The results of the Weibull analysis performed on the three different fibre types, 3-M SSG, PRD-166 and P-55, are shown in Table III. A comparison of the cumulative fibre strength distributions for the three fibre lots evaluated in this study is shown in Fig. 3. Although differing in the strength level, the distribution of the lots of PRD-166 and P-55 fibre studied are similar. The general strength level of the SSG fibre, however, is much higher than either P-55 or PRD-166, even though its cumulative distribution is wider. The PRD-166 and P-55 fibres are well developed and defects leading to the low-end distribution have been eliminated. The 3 M SSG fibres are derived from a new technology and defects leading to the low-end strength populations are still being identified and related to the process. These properties are considered to be evolutionary and the overall excellent properties measured here will improve as defects representing the low end of the Weibull distribution are identified and eliminated from the process.

The limiting-strength parameter σ_0, derived from the Weibull analysis, can be considered to be the fundamental defect-free strength of a given material. A value of 17.6 was derived from these data. It is interesting to note that if the ultimate-strength-limiting defect in a ceramic body is considered to be the grain layer in the cross-section, and it is assumed that the fracture toughness of alumina is 4.5 MPa $m^{1/2}$ and if a penny-shaped-crack-fracture toughness relationship is assumed, then the ultimate SSG fibre strength is calculated to be 16.3 MPa $m^{1/2}$, which is in good agreement with the Weibull-analysis result.

TABLE I Parameters for pressure infiltration casting

Preheating time at T_m and T_p	64 min
Melt temperature T_m	740 °C
Temperature inside mould T_m	666 °C
Temperature outside mould	734 °C
Infiltration pressure	5.5 MPa (800 p.s.i.)
Cooling rate; 720 ⇒ 500 °C	7.3 K min^{-1}

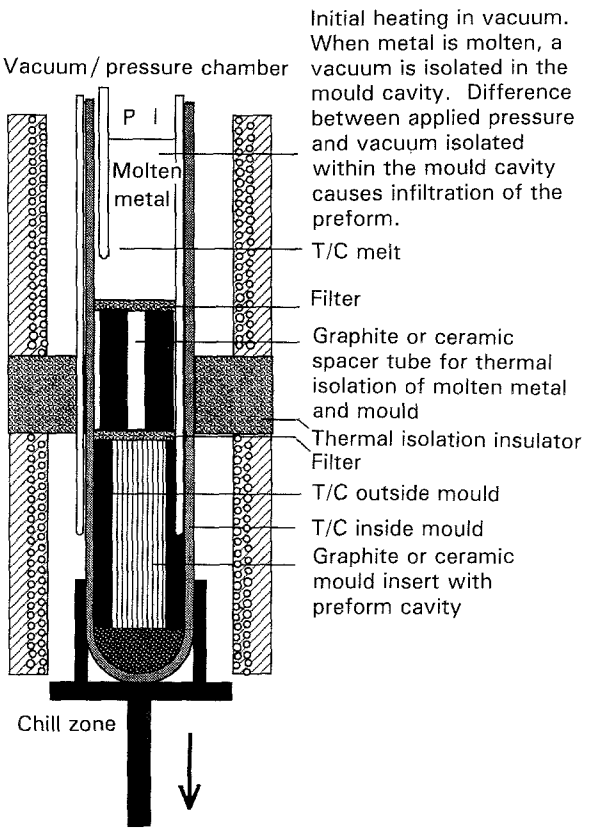

Figure 2 Mould set-up for top-fill infiltration casting process (patent pending to the PCAST corporation).

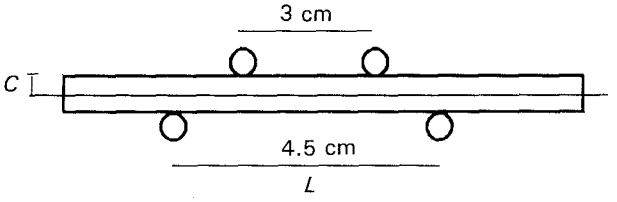

TABLE II Four-point bend test: $\sigma = (M \times C)/I$ where $I = (b \times d^3)/12$ and $M = (1/6) \times P \times L$. Cross-head speed = 0.01 inch min^{-1}

Sample	Vol. fibre (%)	Strength (GPa)	Strength (k.s.i.)	Strength ROM (k.s.i.)	ROM (%)
A	55	0.887	123.2	1.78 GPa (248)	49
B	55	0.683	94.8	1.78 GPa (247)	38

TABLE III Weibull parameters and average fibre strengths for 3M SSG (alumina), DuPont PRD-166 (zirconia-stabilized alumina) and Amoco P-55 (pitch-derived graphite) fibres

Type of fibre	Fibre diameter μm	Weibull modulus m	σ_0	$\bar{\sigma}$ (k.s.i.)	$\bar{\sigma}$ (GPa)	var(σ)
PRD-166	20	4.9286	7.1783	215.3	1.55	0.12535
P-55	10	5.6434	9.825	313.9	2.26	0.20934
3M-(SSG)[a]	10	5.0005	17.59	455.6	3.28	0.59411

[a] Lot 1694-108-14 : 10 # 2

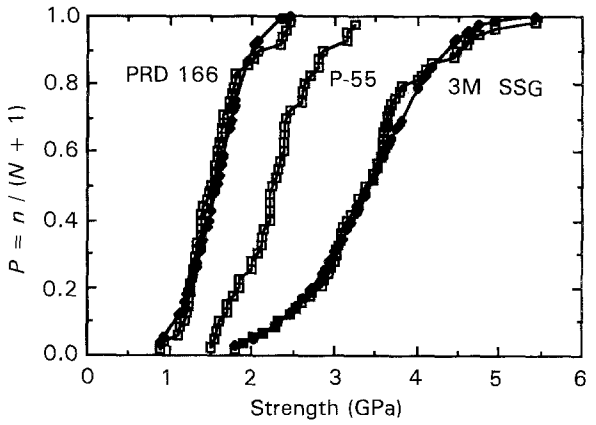

Figure 3 Weibull distributions of the 3M SSG, P-55, and PRD-166 fibre lots: (□) $P = n/(N + 1)$, and (◆) P calculated.

If it is assumed that all the fibres had the same density of flaws, it could be shown that the strength of the fibres would be related to the test length by the relation [4, 5]

$$\sigma_i = \left[\frac{1}{wL_iC}\right]^{1/m} \quad (5)$$

where $w = \pi d_i$, L_i is the test length, $C = (\sigma_0^m \pi d_i^2)^{-1}$ and m is the Weibull parameter.

Inserting the data of the fibres under study in the left-hand side of Equation 5, fibre strengths of 3.67 and 2.45 GPa are obtained for the 3M alumina fibres and for the P-55 fibres, respectively. These calculations are in agreement with the experimental data obtained and show that the fibres are not badly damaged during the testing. Since the value obtained from Equation 5 for the P-55 fibres is closer to the experimental result than for the 3M fibres, it can be deduced that the 3M fabrication process produces fibres whose density of flaws is less regular than for P-55 fibres. This is because this process is brand new.

3.2. Composite strength measurements

The test results are shown in Table II. The strengths obtained are considerably below rule of mixtures (ROM) calculations based on average-fibre-strength measurements. The measured strengths correlate more nearly to the strength of the fibres at the low-strength-end of the Weibull distribution [6]. The results obtained with the 3M fibre reinforced A-1100 aluminium and other samples reinforced with the other two characterized fibres are shown in Table IV. It is possible that fibres were damaged during preform preparation or by chemical interaction with the matrix. This will be evaluated further by dissolving the matrix and tensile testing the liberated fibres.

TABLE IV Composite flexure strengths and calculated fibre strength at the ultimate strength of 55 v/o for SSG, P-55 and PRD-166 reinforced Al(1100)

Sample	Composite strength (GPa)	Average fibre stress at failure (GPa)
3M-SSG	0.887	1.61
P-55[a]	0.729–0.782	1.33–1.42
PRD166[b]	0.5	0.91

[a] From Cornie *et al.* [7].
[b] From [2]

Following Argon's [4, 5] statistical study of composites fracture, the composite strength in tension, σ_c, for 0.55 volume-fraction composites can be calculated

$$\sigma_c = f\left[\Gamma(1 + 1/m)\frac{w\delta[K_3^m - 1]}{m^2\pi d_i L_i \sigma_i^m k}\right]^{-1/m+1} \quad (6)$$

where f is the volume fraction (0.55 in this study); m is the Weibull modulus; $w = \pi d_i$; δ is the statistical ineffective length; L_i is the test length of the fibres; K_3 is the stress-enhancement factor of aluminium (= 1.335); k is the yield-strength-in-shear of aluminium (20 MPa from the "Metals handbook", Vol. 2, tenth edition, American Society for Metals, Metals Park, Ohio; σ_i is the average strength of the fibres (from Equation 3); and d_i is the diameter of the fibres.

Choosing $\delta = 0.7$ mm, based on shear-lag analysis, to take into account the damage incurred by the fibres during the manufacturing process gives

$$\sigma_c = 0.94 \text{ GPa}$$

This result compares well with the experimental results from four-point bend tests of ~ 0.89 GPa. This result shows the importance of fibre distribution on the strength of strongly bonded composite systems. The reduction of interface strength through the deposition of weakly adherent coatings [8] would isolate the fibre from the stress intensifications resulting from defects created by the fracture of a neighbouring fibre and would result in a composite strength closer to ROM values.

The same calculations can be applied to the Al(1100)/P-55 composites. They yield a composite strength of 0.85 GPa from Equation 6 when $\delta = 0.8$ mm. Since aluminium does not wet the carbon, a higher δ has been chosen than for the Al/Al_2O_3 system. This value also agrees with the experimental results. Indeed an Al(1100)/55-v/o-P-55 composite

strength was measured at 0.78 GPa for similarly processed material [9]. The strength of these composites was shown to depend upon the degree of chemical interaction between the fibre and the matrix and the resultant fibre-strength-degradation during infiltration.

3.3. Transverse strength

A 0.55 volume fraction specimen was prepared with the fibres aligned transversly to the tensile testing axis. The experimental stress–strain curve is shown in Fig. 4. The ultimate strength was 50 MPa (7.3 k.s.i.). The parabolic behaviour of the early portion of the stress–strain curve is due to work hardening of the matrix. Handbook values of 1100 Al indicate a yield strength of ~70 MPa, (10 k.s.i.). Although the stress–strain curve indicates considerable matrix deformation, the scanning electron microscopy (SEM) fracture

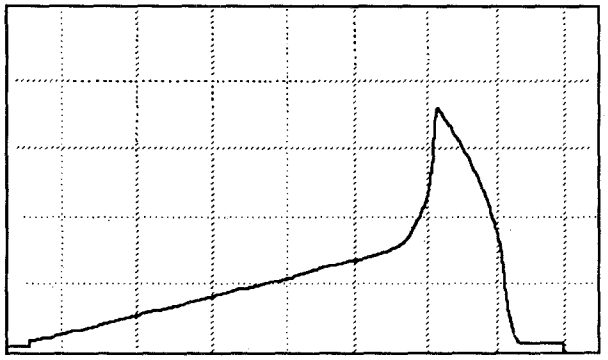

Figure 4 Transverse strength for a 55 v/o SSG reinforced 1100 Al composite measured on an Instron machine: Load cell = 1000 lb, cross-head speed = 0.01 in min^{-1}; σ_{max} = 50 MPa (7.3 k.s.i.), (strength of 1100 Al = 70 MPa).

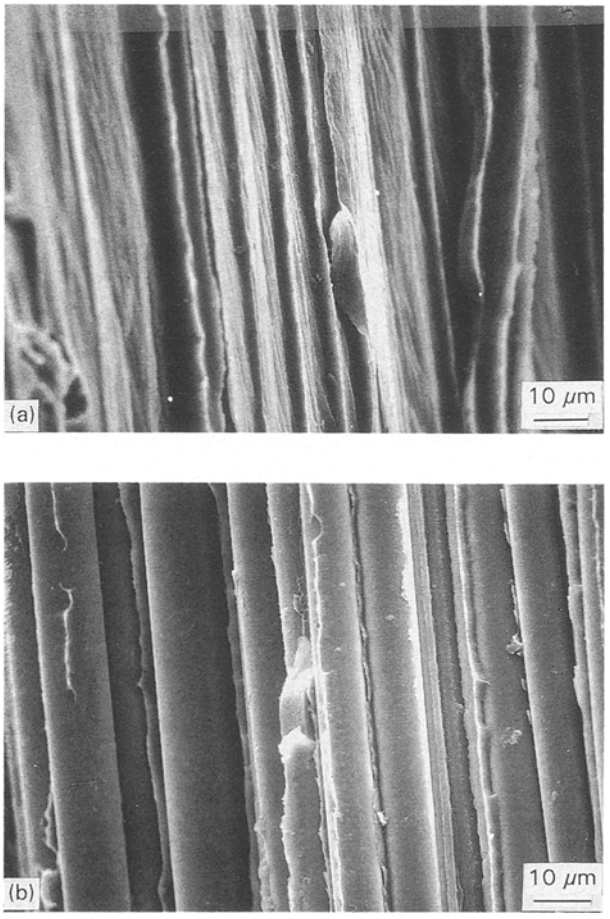

Figure 5 Transverse test specimen fracture surfaces: (a) matrix with fibres pulled out, and (b) fibre surfaces after decohesion from the matrix.

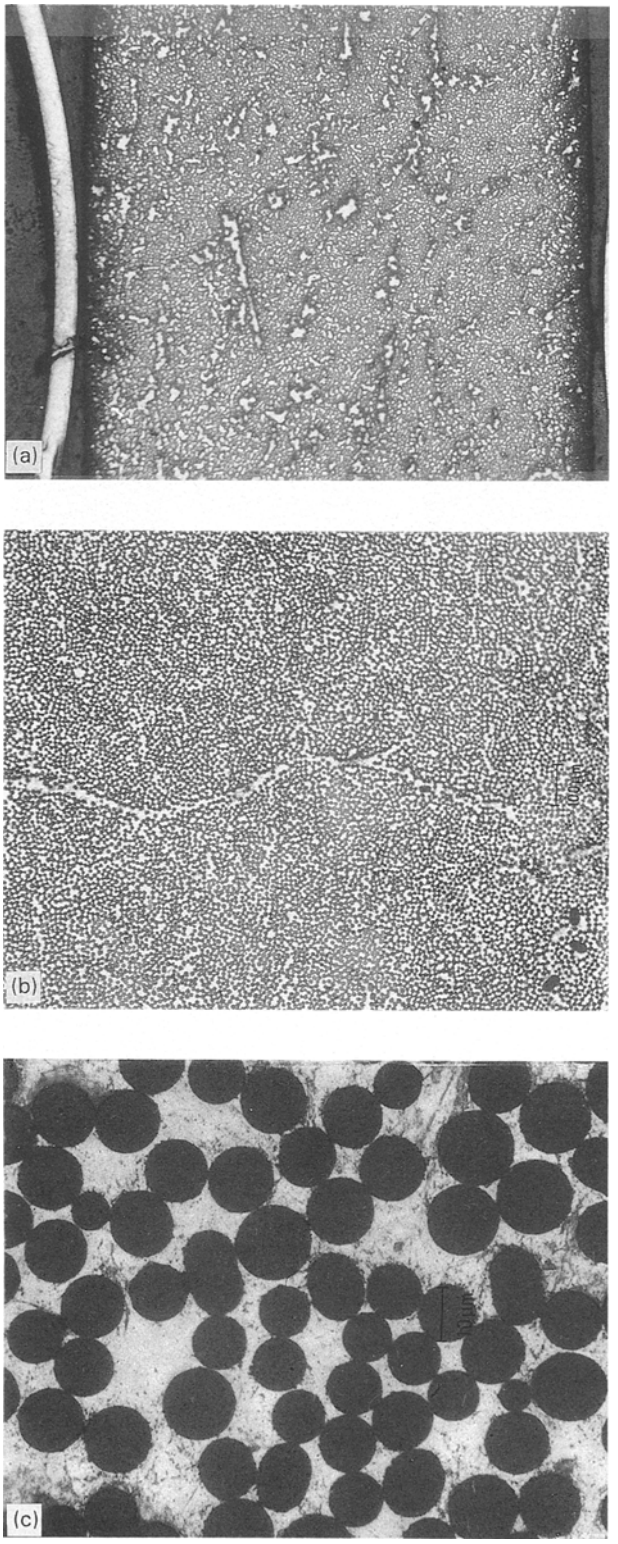

Figure 6 Metallographic sections at low magnification: (a) cross-section of infiltrated flexure test bar; (b) veining due to fibre rearrangement during infiltration; and (c) metallographic section showing fibre distribution, fibre diameter variations and complete infiltration into fibre contact regions.

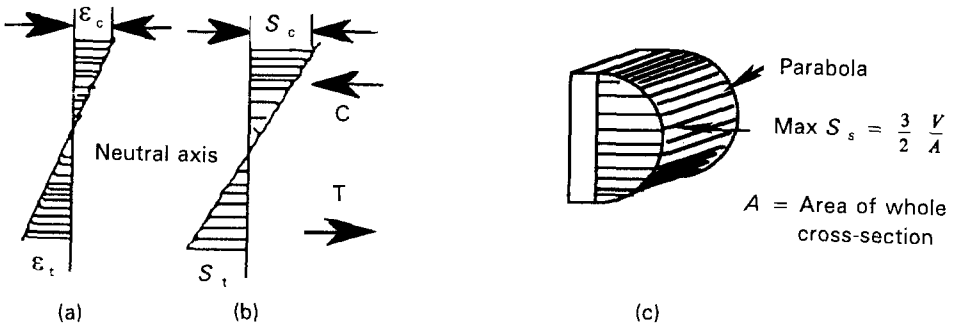

Figure 7 Stress distribution in the sample during the four-point bend test: (a) strain diagram, (b) stress diagram, and (c) variation in shearing stress across a rectangular section.

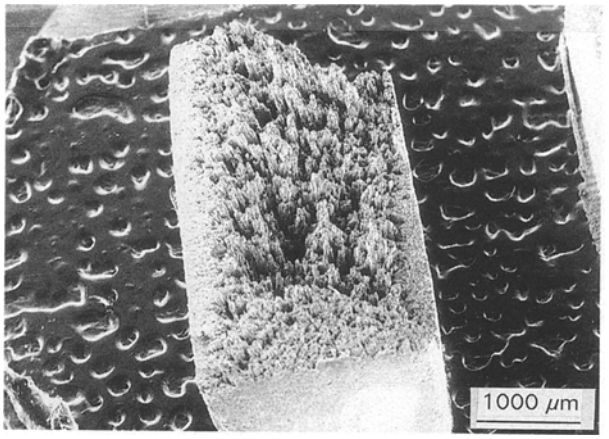

Figure 8 General view of the fracture surface. Compare the planar fracture at the tensile surface with the pull-out–like fracture in the central interlamillar shear-dominated region.

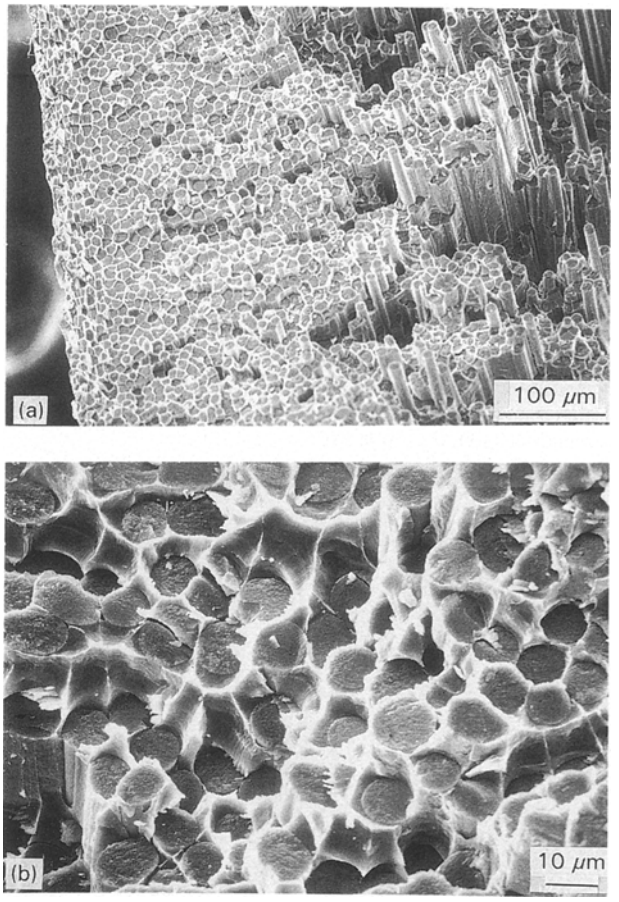

Figure 9 (a) planar transfibre fracture at a tensile-dominated region. (Low magnification). (b) detail at high magnification.

surfaces shown in Fig 5a and b indicate that decohesion of the fibre matrix interface also took place along with matrix deformation. According to the treatment of Cornie, Argon and Gupta [9], the interface must have been sufficiently strong to localize fracture in longitudinal tension but weak enough to fracture at the interface during transverse testing.

3.4. Metallographic and fracture-surface studies

3.4.1. As-cast metallography

The optical metallographs of Fig 6a and b show some rearrangement of fibres during infiltration. The features in Fig. 6a indicate local channels where the fibres are moved aside by the inrushing liquid. This rearrangement occasionally takes the form of a vein when viewed in cross-section as in Fig. 6b. Figs 6a and b with the optical micrograph in Fig. 6c shows complete infiltration, even into the regions where the fibres are in near contact.

3.4.2. SEM fractography

The fracture features can be interpreted by referring to Fig. 7 which indicates the state of tensile and shear stresses in a flexure specimen. Tensile stresses are maximum at the top (tensile) surface where shear approaches zero. At the neutral axis, the tensile stress is zero and the shear stress is a maximum. Fig. 8 is a low-magnification SEM fractograph of the entire fracture surface of a flexure specimen. The fracture surfaces near the tensile and compressive surfaces of the flexure fracture are planar with no evident fibre pull-out as shown in Figs 9a and b. This behaviour is expected in composites with strongly bonded interfaces [9, 10]. The central region of the flexure specimen shows what appears to be fibre pull-out (Fig. 10a). However, SEM examinations of the fibres from the central region, such as in Fig. 10b, show the matrix to be strongly adherent. Since these SEM micrographs were taken from the central region, this should be interpreted as interlamellar shear which predominates near the neutral axis rather than pull-out. SEM observation of the transverse fracture surface shows that

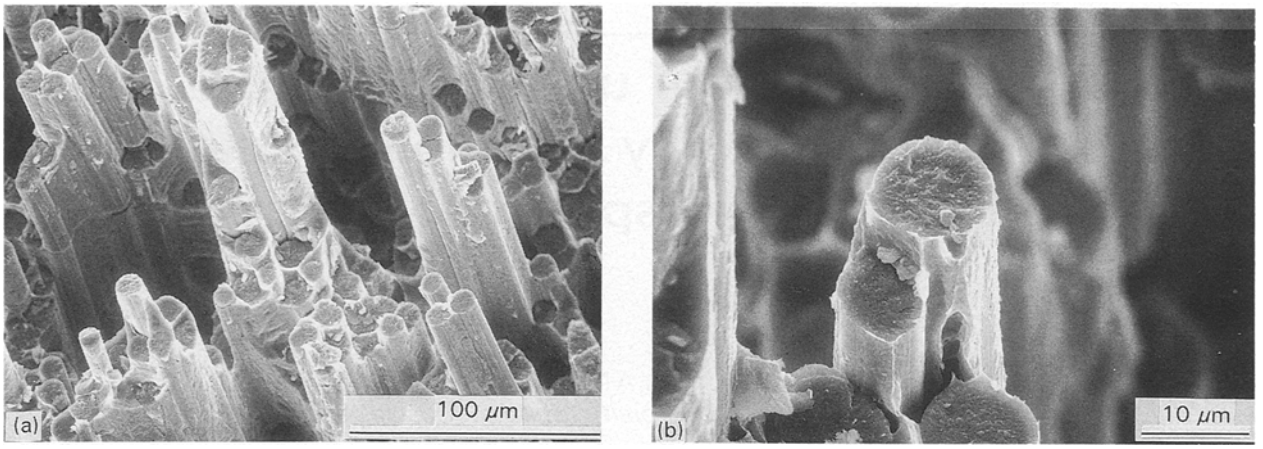

Figure 10 (a) Central interlamillar shear-dominated region of the sample showing apparent fibre pull-out, and (b) further detail, showing complete adhesion of aluminium to the entire fibre surface in the central interlamillar-shear-dominated region of the flexure specimen.

there has been decohesion between the matrix and the fibres (Figs 4a and b). However, some fibres seem to be coated with the aluminium matrix. Interface decohesion and void formation are often found in materials with second-phase inclusions in a plastic matrix [11–13].

4. Conclusions

1. Weibull distributions were obtained for the newly developed, and still evolving, 3M SSG Alumina fibre. These results were compared to the AMOCO P-55 carbon fibre and the PRD-166 alumina fibre produced by DuPont, both of which are considered to be developed and commercially available fibres. The 3M fibre was clearly stronger than the commercial fibres evaluated. However, there was a wider strength distribution.

2. It has been shown that the strength of these strongly bonded composites depends upon the strength of fibres in the lower portion of the Weibull distribution.

3. The 3M SSG fibre is newly developed and the process is still evolving. Further improvements in strongly bonded composites fabricated with this fibre would result from a narrowing of the strength distribution, which is the same as eliminating a certain class of defects resulting from fibre processing.

4. The use of weakened interfaces could serve to increase the composite strength to ROM values based on average fibre strengths.

Acknowledgements

The authors are grateful to the 3M corporation for donating the fibres used in this study. Support for this study was provided by the IST/SDIO under an Office of Naval Research (ONR) contract (Contract N00014-90-J-1812). Additional ONR support for Professor Argon's contribution was made under contract N00014-89-J-1604. One of us (CL) was supported by the SIR/Montedison. Additional financial support was also obtained from the Industrial Consortium for Inorganic Composites which supported a portion of the salary of one of the authors (JC). We had fruitful discussions with Dr David Wilson of 3M on the handling of the SSG fibre. We appreciate the continuing interest of Dr Steven G. Fishman in these processing and interface-related projects.

References

1. Dr D. WILSON, 3M Inc., Private communication.
2. G. K. LEWIS and J. K. ROMINE, The Thirty-Second SAMPE Symposium, Anaheim, CA, April 7, 1987.
3. H. T. CORTER in "Modern composite materials", edited by L. J. Broutman and R. H. Brock (Addison-Wesley, Reading, MA 1967).
4. A. S. ARGON, in "Treatise on materials science and technology", Vol 1 (Academic Press, New York, 1972) p. 79–114.
5. A. S. ARGON, Statistical Aspects of Fracture in "Fracture and Fatigue", Vol 5, in the series, *Composite Materials*, edited by J. L. Broutman and R. H. Krock (Academic Press, New York, 1974).
6. R. K. EVERETT and R. J. ARSENAULT, "Metal matrix composites: Processing and interfaces" (Academic Press, New York, 1991).
7. B. W. ROSEN and N. F. DOW in "Fracture", Vol 7, edited by Liebowitz (Academic Press, New York, 1972) p. 611–73.
8. J. A. CORNIE, A. S. ARGON and V. J. GUPTA, *MRS Bulletin*, **16** (1991) p. 32–8.
9. J. A. CORNIE, A. S. ARGON and V. J. GUPTA, in "Ceramic Transactions", Vol. 19, edited by Michael D. Sachs, (1991) p. 215–815.
10. V. J. GUPTA, PhD thesis Massachusetts Institute of Technology (1989).
11. A. S. ARGON, J. IM and R. SAFOGLU, *Metall. Trans. A***6** (1975) 825–37.
12. A. S. ARGON, J. Engng. *Mater. Technol.* **98** (1976) 60.
13. M. F. AMATEAU and D. L. DULL in Proceedings of Symposium by TMS–AIME, edited by J. A. Cornie and F. W. Crossman (American Society for Metals), Metals Park, OH (1978) p. 336.

Received 12 February
and accepted 10 December 1992